Project Ref.: 312495

PROJECT

SOLARNET

TITLE

CORRECTION FOR IMAGE MOTION FOR THE FULL DISK IMAGING SPECTRO-POLARIMETER (FDISP)

WORK-PACKAGE (DELIVERABLE NR)

WP8: SOLAR PHYSICS RESEARCH INTEGRATED NETWORK GROUP (SPRING)

AUTHORS LIST

Name	Function
Dirk Soltau	WP8: Project Scientist
Markus Roth	WP8: Project Leader

APPROVAL CONTROL

Control	Name	Organization	Function	Date
Prepared	Dirk Soltau	KIS	WP8: Project Scientist	08/11/2021
Revised	Markus Roth	KIS	WP8: Project Leader	22/12/2021
Approved				
Authorized				

DOCUMENT CHANGE RECORD

Issue	Date	Change Description
01	26/10/2021	Initial Issue
02	08/11/2021	Revisions by authors
03	22/12/2021	Finalization of document by authors

TABLE OF CONTENTS

SUMMARY

1. INTRODUCTION

The instrument under consideration will perform spectral scanning by changing the air gap in one or two Fabry-Pérot interferometers. That means that each scan step will be done at a different time. If the image shifts between scan steps the data reduction becomes very tedious because the sequentially taken images must be stacked properly. In addition, also demodulating the polarimetric data involves combining data taken at different times. If the solar image is not stable on the detector within a certain margin the science requirements which ask for 10 m/s velocity sensitivity and 10 G magnetic sensitivity may not be reached.

A system will be designed according to requirements and/or specifications. In many cases the difference between these two expressions is not clear and their misleading use can cause confusion and misunderstanding. In this document we want to distinguish between

- **Requirements**: These are performance characteristics which are needed to fulfill the scientific goals which have been defined in a science requirement document. They define a design goal. It may be that requirements are unrealistic because they contradict fundamental limitations.
- **Limitations**: These are properties of the system which work against the requirements. Typical limitations are given by errors in the system. Any real system contains errors which should be recorded in an error budget. There are fundamental errors like photon noise or less fundamental errors like manufacturing errors.
- **Specifications**: These are properties of the system or its components which are real and (in the best case) proven.

2. REQUIREMENTS

In this document we concentrate on the effect of image shift on the detector. For this the following requirements are applicable:

We want to design a system which can perform the following tasks

- Do the measurements with a pixel resolution of 0.5 arcsec. According to the Nyquist theorem this corresponds to a spatial resolution of 1 arcsec;
- Measure Doppler velocities in many (e.g. 15) spectral lines with a sensitivity of 10 m/s;
- Measure the full Stokes vector with a sensitivity of 10 G for the vertical field in several magnetic lines.

In the following sections we shall discuss how these requirements relate to limitations and specifications.

3. LIMITATIONS

3.1 Fundamental limitations

3.1.1 Noise level

In order to deduce requirements for the image stability we looked at HMI data as a reference: HMI has the same pixel resolution as the planned instrument (0.5 arcsec/px) but operates under space conditions: There is no seeing and a neglectable mechanical jitter.

As an example, we took the following file:

hmi_v_45s_2020_12_20_00_01_30_tai_dopplergram.fits

which is available from NASA' Solar Dynamics Observatory (SDO) and was recorded by the Helioseismic and Magnetic Imager (HMI) on board of this space mission.

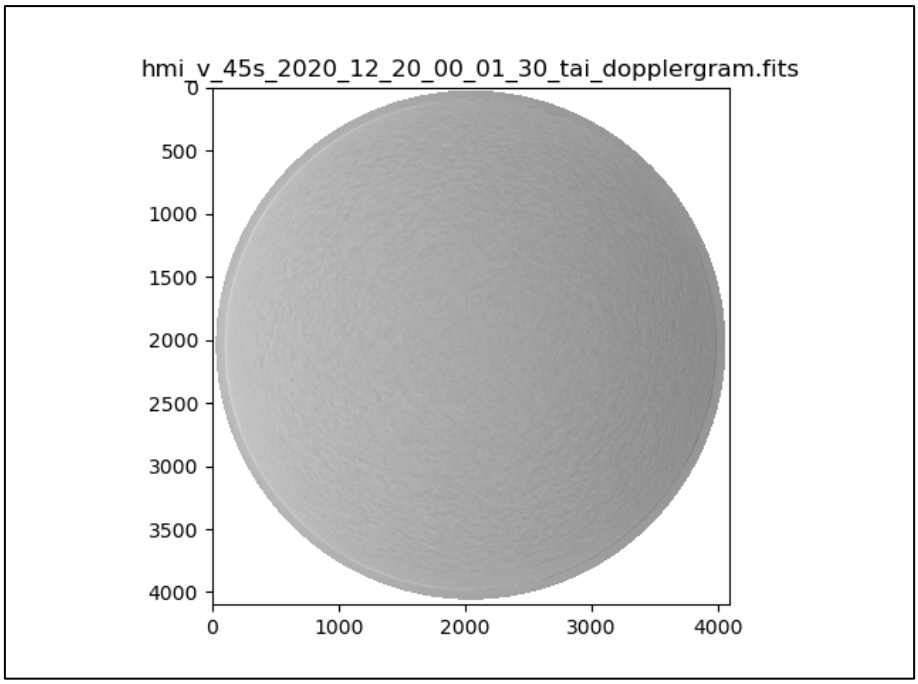

Figure 1: HMI Dopplergram

We looked at the one-dimensional power spectrum and the autocorrelation function across a horizontal scan omitting the outer 100 arcsec of the image. See Figure 2.

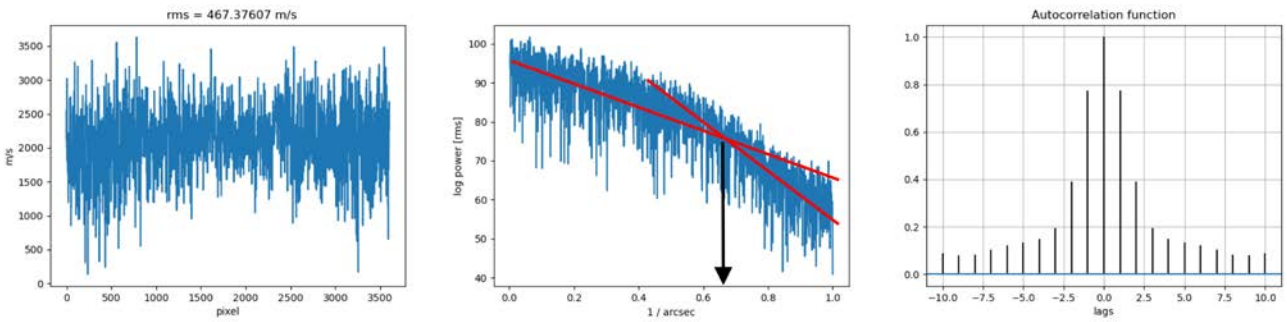

Figure 2: Horizontal velocity scan, log power spectrum, and autocorrelation function

From the power spectrum (centre panel) we see that the cut-off frequency for noise happens roughly at structure sizes smaller than 1/0.65 = 1.5 arcsec. This is in agreement with the drop of the autocorrelation function which reaches 0.2 at a lag of three pixels.

We conclude that with our instrument we cannot expect velocity signals at spatial scales smaller than 1.5 arcsec corresponding to 3 pixels. We consider this as a fundamental limitation.

Deduced requirement:

Assuming a Gaussian error distribution we end up with a stability requirement of ± 1.5 pixel (P-V) corresponding to 0.5 pixel = 0.25 arcsec (rms)

3.1.2 Diffraction limit

As it is discussed elsewhere the aperture of the telescope will be limited by the (useful) diameter of the etalon(s) which is assumed to be 120 mm.

Using the well-known formula for the angular resolution as a function of wavelength λ and aperture D

$$\Delta\alpha = 1.22\frac{\lambda}{D}[rad]$$

We obtain 1 arcsec (2 pixel) resolution at 500 nm and 2 arcsec (4 pixel) at 1000 nm wavelength.

These numbers are roughly the same as those from the HMI analysis and confirm our image stability requirement of 0.25 arcsec (rms)

Deduced requirement:

Even under ideal conditions we cannot expect significant signals at spatial scales below appr. 1.5 arcsec. So the hardest meaningful requirement for image stability is 0.25 arcsec (rms)

3.2 Other limitations and their sources

We see the following sources for image jitter:

1. Seeing
2. Wind force
3. Internally induced vibrations.

3.2.1 Seeing

Turbulence deforms the wavefront as the light passes the earth's atmosphere. This is because the index of refraction changes as a function of height and time. Although the details of this process are complex the overall properties can be described by two parameters:

1. The so-called Fried parameter r_0 for the spatial domain. Its value is typically given in cm. Typical numbers: bad seeing: $r_0 < 5$ cm, good seeing $r_0 > 10$ cm, very good seeing $r_0 > 20$ cm.
2. The so-called Greenwood frequency f_G for the time domain. Its value is typically given in Hz. Typical value: $f_G < 200$ Hz (good seeing), $f_G > 500$ Hz (bad seeing). It can be estimated as the ratio of wind speed (in the height of the turbulence layer) to r_0.

The seeing effects depend on the ratio of telescope diameter D to r_0, as well as the wavelength λ . A widely used formula for the seeing induced image jitter is the following:

$$rms\ jitter = \sqrt{0.182\ \lambda^2 D^{-1/3} {r_0}^{-5/3}}$$

For a 120 mm telescope we obtain Figure 3. For average seeing we would expect a rms jitter of about 1 arcsec.

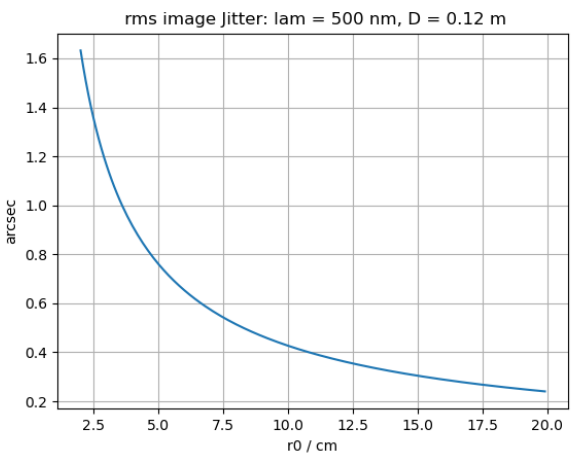

Figure 3: Theoretical image jitter inside an isoplanatic patch.

But these formulae tend to fail for small D/r_0 ratios. In addition, they refer to the so-called isoplanatic patch which is the size of the FOV over which the wavefront can be assumed to be flat. The size of the isoplanatic patch is in the order of some tens of arcsec which is much smaller than our FOV (roughly 2000 arcsec). This leads to an averaging over many isoplanatic

patches and will reduce the mean jitter of the whole disk significantly. The seeing will show up e.g. as an undulated solar limb while the average position of the whole disk will remain quite stable.

We don't know yet the final site selection but from the GONG sites we can assume different qualities for different sites. We think that a typical r_0 between 5 and 10 cm is realistic.

If granulation has to be detected (spatial frequency appr. 0.5/arcsec, intrinsic contrast appr. 14%) the modulation transfer function at this frequency should exceed 0.2, so that the image contrast is beyond 2% at that frequency.

The atmospheric MTF can be estimated with the relation

$$MTF_{atm}(\nu) = exp\left[-3.44(\lambda f \nu / r_0)^{5/3}\right]$$

with

ν = spatial frequency
f = system focal length

Figure 4 shows the combined effect for diffraction and seeing.

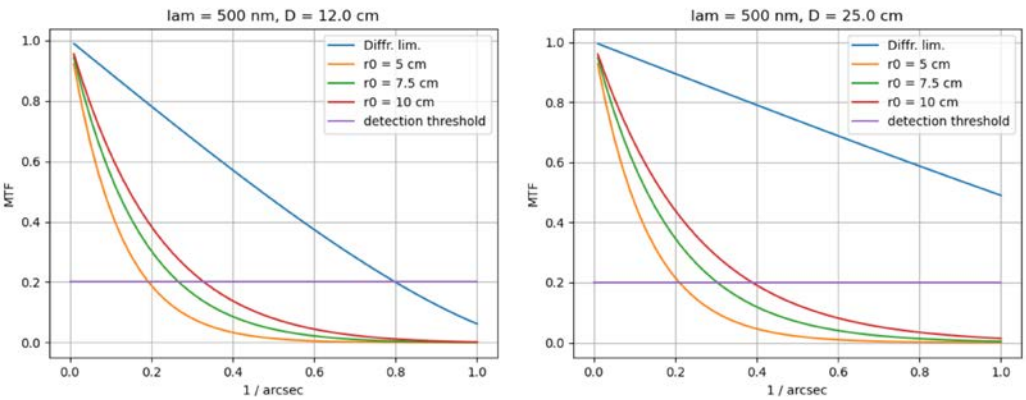

Figure 4: MTF for diffraction alone and diffraction plus various seeing conditions. Left panel: 12 cm aperture, right panel: 25 cm.

From Figure 4 we learn that under nominal conditions we shall be seeing limited. Even if we double the aperture (right panel) we do not gain a lot of performance. In practice our resolution in terms of contrast detection threshold will be about 2 to 3 arcsec.

Conclusion:

The limitations by seeing are probably the worst offenders w.r.t. the resolution requirements

3.2.2 Wind force

The wind forces on the turret may be the dominant effect for image jitter. We estimate them using the following parameters:

- Wind speed: 10 m/s
- Projected area: 0.5 m^2

Using standard formulae, we obtain typical wind forces in the order of 50 Newton on the turret (TBC) which lead to certain image shifts depending on the stiffness of the structure. The stiffness will only be known after a finite element analysis of the final design.

The temporal behaviour depends on the wind spectrum. This is very local depending on the winds and the shape of the landscape. But in general, it is much slower than the seeing effects and the frequencies are in the order of less than 1 Hz (van der Hoven wind spectrum).

Conclusion:

The exciting wind forces are relatively slow but strong. The excited amplitudes are not yet known. See Section 6.

3.2.3 Internally induced vibrations

The system consists of a structure which will have a wide spectrum of eigenfrequencies. These frequencies will be much higher than the wind frequencies. Nevertheless, an excitation of resonance frequencies may occur. In addition, there may be forced excitations by movable parts like cooling fans. These may have power line frequencies (50 Hz) or higher modes.
Here we may expect small amplitudes but high frequencies (up to hundreds of Hz)

Conclusion:

To obtain a closed bandwidth of more than 100 Hz we need a system with eigenfrequencies larger than 1 kHz.

4. SPECIFICATIONS FOR A TIPTILT CORRECTION

In this Section we shall introduce a technical solution for a tiptilt correction system and present its specifications.

Figure 1 shows the FDISP baseline design.

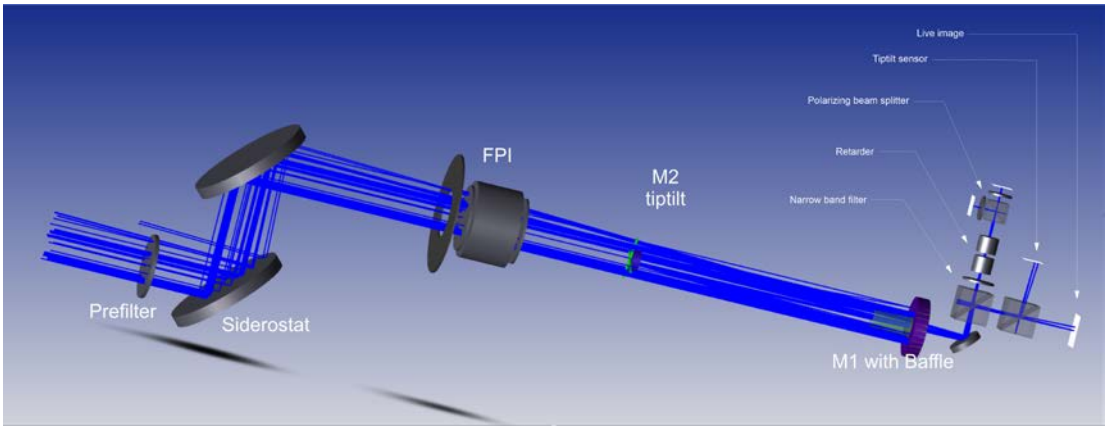

Figure 5: Optical layout FDISP

A non-polarizing beam splitter reflects part of the light to the branch where we place the tiptilt sensor behind the reflected part of another beam splitter (see Figure 5). A relay optic demagnifies the primary image to fit on the fast sensor camera.

4.1 The sensor camera

As a candidate for the sensor camera we selected a Mikrotron Eosens 3CL camera. This camera with camera link interface provides 1280 x 1024 images with 1280 x 1024 pixels at a rate of 600 frames per second. See Figure 6.

Figure 6: The TT sensor camera candidate (Image courtesy: IMAGEOPS, USA; MIKTROTRON GmbH, Germany)

Technical specifications are shown in Figure 7.

Technical Data

(More detailed specifications are available on request)

	EoSens® 3CL (monochrome / color)
Resolution	3 Mpix
Active pixels	1,690 x 1,710 px
Interface	Camera Link® Full
Frame rate (8 bit)	285 fps
Sensor	LUPA3000
Sensor type	CMOS global shutter
Sensor format	1"
Active sensor area (H x V)	13.57 x 13.68 mm
Pixel size	8 x 8 µm
Sensitivity (mono)	3.81 V/lux*s @ 550nm
Color depth	8 bit
Dynamic range	80 dB
Shutter time (steps)	1 µs
Shutter time range	1 µs – 1 s
GPIO	STRB
Mount options	C-Mount / F-Mount
Dimensions (W x H x L w/o mount)	63 x 63 x 52 mm
Weight (C-Mount)	300 g
Power consumption	7 W
Power supply	8 – 24 V DC
Camera body temperature	+5 °C ... +50 °C
Shock / Vibration proof	70 g / 7 grms
Conformity	CE / RoHS / Camera Link®
EMVA 1288 reports	✓

Figure 7: Technical data of a 3CL camera as provided from the data sheet (https://www.imageops.com/image-processing/high-speed-camera/pdf/mikrotron_eosens_3cl_full-CL-dsh.pdf)

The digitization is only 8 bit but from the Kanzelhöhe data (see Section 6) we learned that algorithms to determine the position of the whole solar disk are very robust and sensitive.

Conclusion:

The specifications of the selected camera are in accordance with the requirements

4.2 The tiptilt actuator

The mechano-optical design foresees the secondary mirror M2 as the active element to correct for image shifts.

The corresponding scale factor is

To obtain an image shift of 1 arcsec on the sky, M2 has to be tilted by 8.6 µrad.

The classical solution is to use a piezo driven tiptilt stage.

As a baseline design we selected the S-340 tip/tilt platform made by Physik Instrumente. Figure 8 shows the specifications for the S-340 series.

The most important specifications are

Full range	2 mrad = 230 arcsec on the sky
Resolution in closed loop	0.2 µrad = 0.02 arcsec on the sky
Resonance frequency with 50 mm mirror	1.4 kHz

These specifications are in accordance with the requirements presented in the previous sections.

Specifications

	S-340.ASD / S-340.ASL	S-340.ISD / S-340.ISL	S-340.A0L	S-340.I0L	Unit	Tolerance
Active axes	θ_X, θ_Y	θ_X, θ_Y	θ_X, θ_Y	θ_X, θ_Y		
Motion and positioning						
Integrated sensor	SGS	SGS	-	-		
Tip/tilt angle in θ_X, θ_Y at -20 to +120V, open loop	2	2	2	2	mrad	Min.
Tip/tilt angle in θ_X, θ_Y, closed loop	2	2	-	-	mrad	
Resolution in θ_X, θ_Y, open loop	0.02	0.02	0.02	0.02	µrad	Typ.
Resolution in θ_X, θ_Y, closed loop	0.2	0.2	-	-	µrad	Typ.
Linearity error in θ_X, θ_Y	0.1	0.1	-	-	%	Typ.
Repeatability in θ_X, θ_Y	0.15	0.15	-	-	µrad	Typ.
Mechanical properties						
Resonant frequency in θ_X, θ_Y, unloaded	1.7	1.1	1.7	1.1	kHz	±20 %
Resonant frequency loaded in θ_X, θ_Y (with glass mirror, Ø 50 mm, thickness 5 mm, 21 g)	1.4	1.0	1.4	1.0	kHz	±20 %
Resonant frequency loaded in θ_X, θ_Y (with glass mirror, Ø 50 mm, thickness 13 mm, 63 g)	1.0	0.85	1.0	0.85	kHz	±20 %
Resonant frequency loaded in θ_X, θ_Y (with glass mirror, Ø 75 mm, thickness 19 mm, 197 g)	0.55	0.5	0.55	0.5	kHz	±20 %
Distance of pivot point to platform surface	7.5	7.5	7.5	7.5	mm	±1 mm
Platform moment of inertia	18000	54000	18000	54000	g × mm²	±20 %
Drive properties						
Ceramic type	PICMA®	PICMA®	PICMA®	PICMA®		
Electrical capacitance	6 / axis	6 / axis	6 / axis	6 / axis	µF	±20 %
Miscellaneous						
Operating temperature range	-20 to 80	-20 to 80	-20 to 80	-20 to 80	°C	
Housing material	Aluminum	Aluminum	Aluminum	Aluminum		
Platform material	Aluminum	Invar	Aluminum	Invar		
Mass	0.355	0.443	0.355	0.443	kg	±5 %
Cable length	2	2	2	2	m	+100 mm / -0 mm
Sensor/voltage connector	ASD version: D-sub 25 (m) ASL version: LEMO	ISD version: D-sub 25 (m) ISL version: LEMO	LEMO	LEMO		
Recommended electronics	E-727	E-727	E-727	E-727		

Figure 8: Specifications for the S-340 tip/tilt series (table courtesy: Physik Instrumente)

5. SUMMARY AND CONCLUSIONS

We investigated the relation between the image stabilization requirements with respect to the fundamental limitations and the specifications of possible technical solutions.

We conclude that the specifications of the technical solution (sensor and tip/tilt stage) are in accordance with the science requirements. Image stabilization of the whole disk will be possible.

The worst offender which limits the resolution is the seeing at the selected site. Because of the large field of view there is no way to compensate image blurring.

6. APPENDIX: KANZELHÖHE DATA REDUCTION

Even if we can estimate and characterize some jitter properties from theory there is nothing better than real measurements. We looked for some real data and selected the Kanzelhöhe images as a reference for a mature system where we assume that the mechanical stability is similar to our design.

Kanzelhöhe observatory regularly takes full disk images of the Sun. It has no image stabilization system. So by looking at these images we expect to get some information about the behaviour of a real system and to see how a typical image jitter for a full disk telescope without image stabilization looks like.

6.1 The telescope

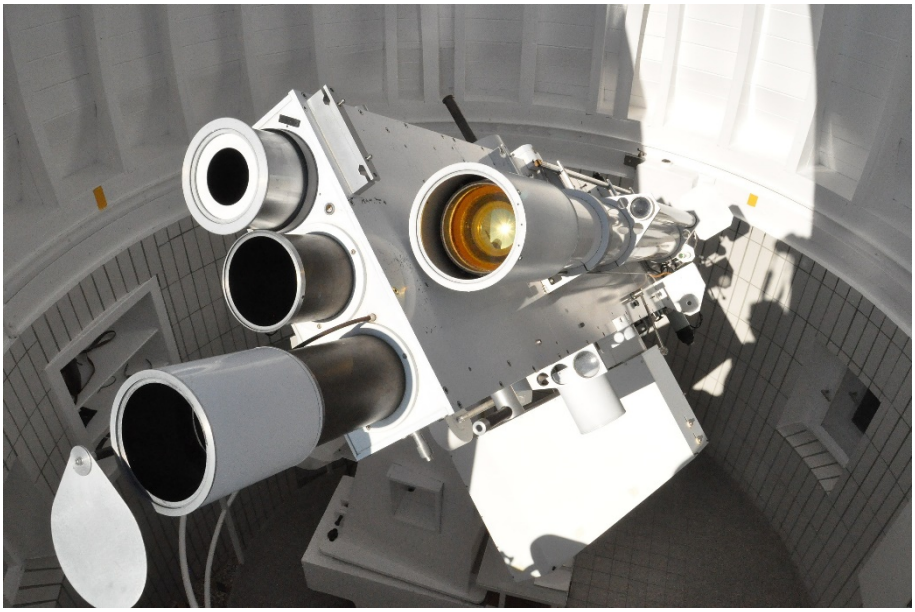

Figure 9: Kanzelhöhe patrol instrument (reference: Pötzi et al., 2015, Solar Physics 290, 951)

The white light telescope is mounted - together with other instruments – on an equatorial mounting inside a small dome. This dome acts as a wind shield as long as the wind does not blow into the dome. In this case vibrations may be excited.

Table 1: Some characteristics of the Kanzelhöhe full disk telescope

Aperture	130 mm
Focal length	1460 mm
Filter pass band	546 nm ± 5 nm
Chip size	2048 x 2048 pixel
Cadence	20 s

6.2 The images

We took the raw images from four days and determined the disk position by calculating the centre of gravity for the whole 2k x 2k image. Figure 10 shows a sample image.

To determine the accuracy of the algorithm we shifted the image by one pixel (1 arcsec) and looked at the differences between the shifted and the unshifted position. Figure 11 shows the distribution. This simple algorithm shows an error distribution of roughly ± 0.1 arcsec.

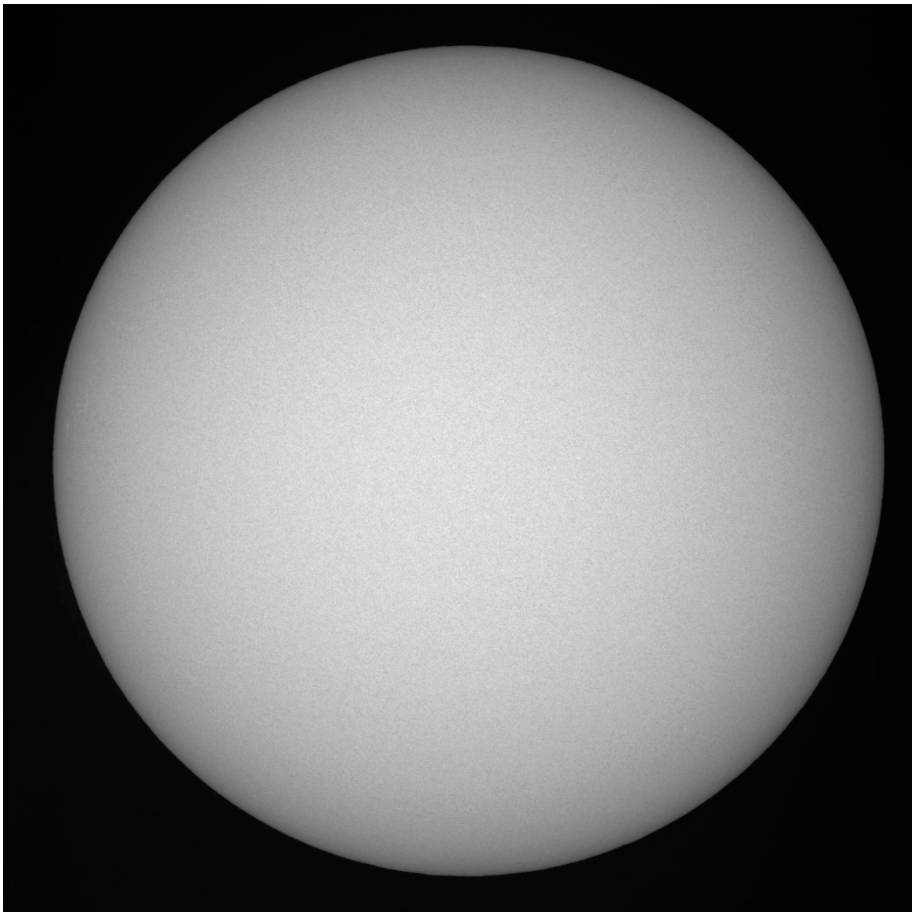

Figure 10: Full disk image dating from 2020-04-10 at 5:57:12 UTC taken at Kanzelhöhe Solar Observatory.

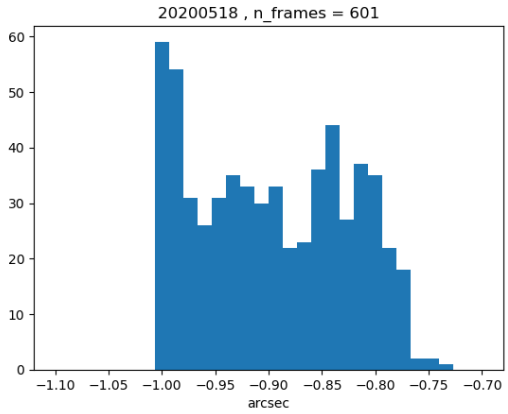

Figure 11: Position distribution for a shift of -1 arcsec

6.3 Results

The following plots show scatter plots and histograms for the telescope view angle w.r.t. to the disk centre. The lower panels show the disk position as a function of time. The measurements give no information about the high frequency behaviour, but it is reasonable to assume that the measurements are statistically independent from each other, since their time distance is 20 seconds. Then the measurements represent the overall behaviour.

We summarize the result as follows:

- The image jitter varies from day to day.

Day	rms x / arcsec	rms y /arcsec
2020-04-10	26	11
2020-04-21	11	11
2020-05-18	16	17
2020-10-09	8	7

These numbers are at least one order of magnitude worse than our requirements.

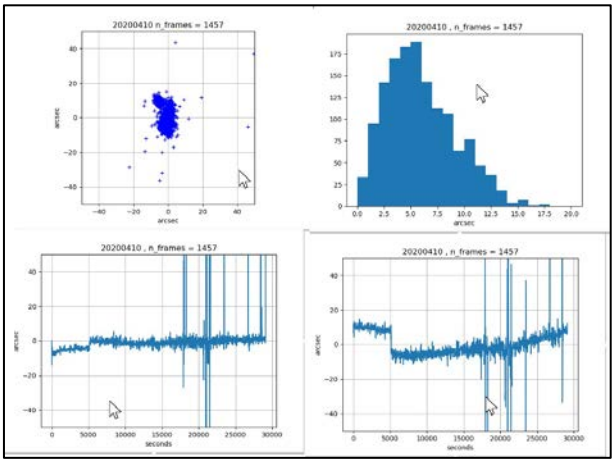

Figure 12: Jitter for 2020-04-10

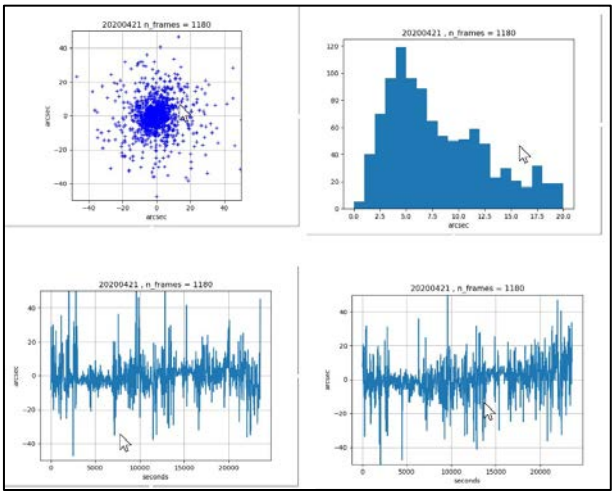

Figure 13: Jitter for 2020-04-21

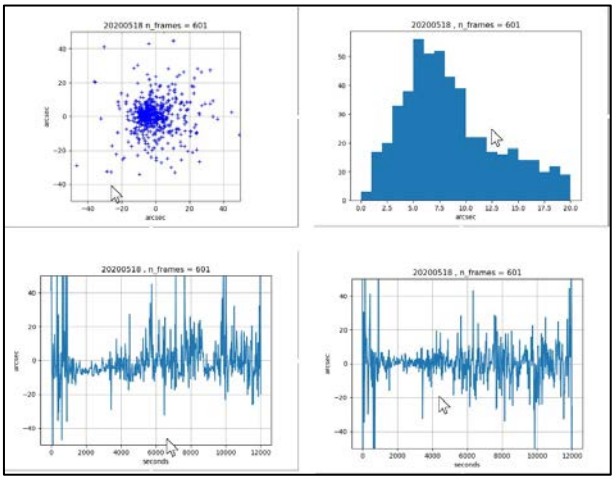

Figure 14: Jitter for 2020-05-18

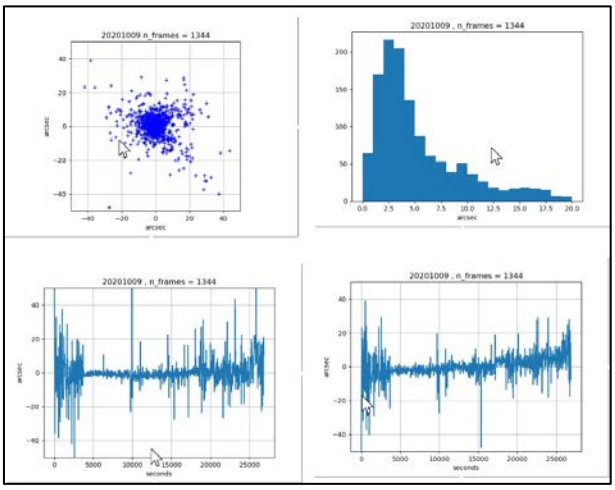

Figure 15: Jitter for 2020-10-09

Taking Kanzelhöhe as a typical example for a full disk telescope, assuming its stability is typical for a full disk telescope, we have to expect image shifts up to ± 50 arcsec.

This is obviously no seeing effect (see Section 3.2.1) but a mechanical wind induced jitter and therefore a low frequency effect (see Section 3.2.2). About the temporal spectrum beyond 0.025 Hz we have no further information. For our project we must assume that the highest frequencies will come from the resonance of the structure.